Random matrix theory and classical statistical mechanics: Vertex models

H. Meyer* and J.-C. Anglès d'Auriac[†]

Centre de Recherches sur les Très Basses Températures, Boîte Postale 166, 38042 Grenoble, France

J.-M. Maillard[‡]

Laboratoire de Physique Théorique et Hautes Energies, Tour 16, 4 place Jussieu, 75252 Paris Cedex, France

A connection between integrability properties and general statistical properties of the spectra of symmetric transfer matrices of the asymmetric eight-vertex model is studied using random matrix theory (eigenvalue spacing distribution and spectral rigidity). For Yang-Baxter integrable cases, including free-fermion solutions, we found a Poissonian behavior, whereas level repulsion close to the Wigner distribution is found for nonintegrable models. For the asymmetric eight-vertex model, however, the level repulsion can also disappear, and the Poisson distribution be recovered on (non Yang-Baxter integrable) algebraic varieties, the so-called disorder varieties. We also present an infinite set of algebraic varieties which are stable under the action of an infinite discrete symmetry group of the parameter space. These varieties are possible loci for free parafermions. Using our numerical criterion, we tested the generic calculability of the model on these algebraic varieties. [S1063-651X(97)14305-7]

PACS number(s): 05.50.+q, 05.20.−y, 05.45.+b

I. INTRODUCTION

Since the early work of Wigner [1] random matrix theory (RMT) has been applied with success in many domains of physics [2]. Initially developed to serve for nuclear physics, RMT proves itself to provide an adequate description to any situation implying chaos. It has been found that the spectra of many quantum systems is very close to one of four archetypal situations described by four statistical ensembles. For the few integrable models this is the ensemble of diagonal random matrices, while for nonintegrable systems this can be the Gaussian orthogonal ensemble (GOE), the Gaussian unitary ensemble, or the Gaussian symplectic ensemble, depending on the symmetries of the model under consideration.

In the last years several quantum spin Hamiltonians have been investigated from this point of view. It has been found [3,4] that one-dimensional (1D) systems for which the Bethe ansatz applies have a level spacing distribution close to a Poissonian (exponential) distribution, $P(s) = \exp(-s)$, whereas if the Bethe ansatz does not apply, the level spacing distribution is described by the Wigner surmise for the GOE:

$$P(s) = \frac{\pi}{2} s \exp(-\pi s^2/4). \tag{1}$$

Similar results have been found for 2D quantum spin systems [5–7]. Other statistical properties have also been analyzed, showing that the description of the spectrum of the quantum spin system by a statistical ensemble is valid not only for the level spacings but also for quantities involving more than two eigenvalues.

In a recent paper [8], we proposed the extension of random matrix theory analysis to models of classical statistical mechanics (vertex and spin models), studying the transfer matrix of the eight-vertex model as an example. The underlying idea is that, if there actually exists a close relation between integrability and the Poissonian character of the distribution, it could be better understood in a framework which makes Yang-Baxter integrability and its key structures (commutation of transfer matrices depending on spectral parameters) crystal clear: one wants to switch from a quantum Hamiltonian framework to a transfer matrix framework. We now present the complete results of our study of transfer matrices, and a detailed description of the numerical method. This work is split into two papers: the first one describes the numerical methods and the results on the eight-vertex model, the second one treats the case of discrete spin models with the example of the Ising model in two and three dimensions and the standard Potts model with three states.

We will analyze a possible connection between statistical properties of the entire spectrum of the model's transfer matrix and the Yang-Baxter integrability. *A priori*, such a connection is not sure to exist, since only the few eigenvalues with the largest modulus have a physical signification, while we are looking for properties of the entire spectrum. However, our numerical results show a connection which we will discuss. We will also give an extension of the so-called ''disorder variety'' to the asymmetric eight-vertex model, where the partition function can be summed up without Yang-Baxter integrability. We then present an infinite discrete symmetry group of the model, and an infinite set of algebraic varieties stable under this group. Finally, we test all these varieties from the point of view of RMT analysis.

This paper is organized as follows: in Sec. II we recall the machinery of RMT, and we give some details about the numerical methods we use. Section III is devoted to the eight-vertex model. We list the cases where the partition function can be summed up, and give some interesting analytical re-

———
*Electronic address: hmeyer@thp.uni-duisburg.de
[†]Electronic address: dauriac@crtbt.polycnrs-gre.fr
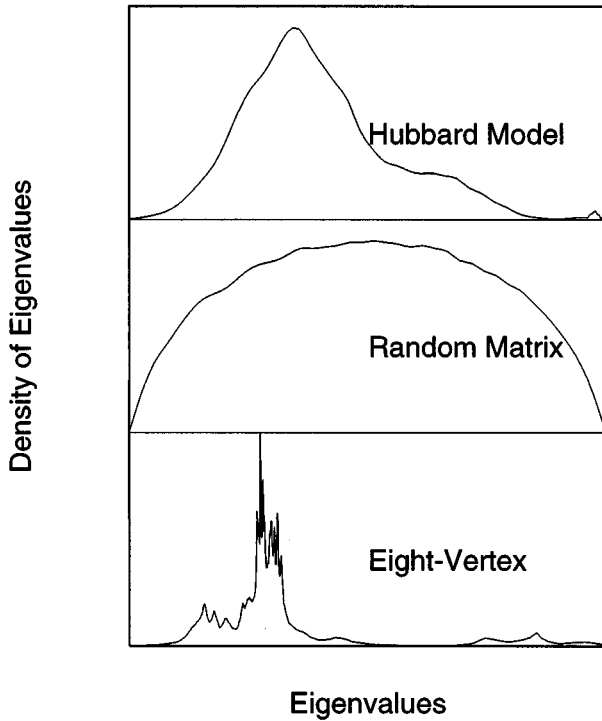[‡]Electronic address: maillard@lpthe.jussieu.fr

FIG. 1. Schematic examples for the density of eigenvalues for the $2d$ Hubbard, GOE random matrices, and transfer matrices of the eight-vertex model.

sults concerning the disorder variety and the automorphy group of the asymmetric eight-vertex model. The numerical results of the analysis of the spectrum of transfer matrices are presented in Sec. IV. Section V concludes with a discussion.

II. NUMERICAL METHODS OF RMT

A. Unfolding of the spectrum

In RMT analysis one considers the spectrum of the (quantum) Hamiltonian, or of the transfer matrix, as a collection of numbers, and one looks for some possibly universal statistical properties of this collection of numbers. Obviously, the raw spectrum will not have any universal properties. For example, Fig. 1 schematically shows three densities of eigenvalues: for a $2d$ Hubbard model, for an eight-vertex model, and for the Gaussian orthogonal ensemble. They have clearly nothing in common. To find universal properties, one has to perform a kind of renormalization of the spectrum, this is the so-called unfolding operation. This amounts to making the *local* density of eigenvalues equal to unity everywhere in the spectrum. In other words, one has to subtract the regular part from the integrated density of states, and consider only the fluctuations. This can be achieved by different means; however, there is no rigorous prescription, and the best criterion is the insensitivity of the final result to the method employed or to the parameters (for ''reasonable'' variation).

Throughout this paper, we call E_i the raw eigenvalues and ϵ_i the corresponding unfolded eigenvalues. Thus the requirement is that the local density of the ϵ_i's is 1. We need to compute an averaged integrated density of states $\overline{\rho}(E)$ from the actual integrated density of states,

$$\rho(E) = \frac{1}{N} \int_{-\infty}^{E} \sum_i \delta(e - E_i) de, \tag{2}$$

and then we take $\epsilon_i = N\overline{\rho}(E_i)$. To compute $\overline{\rho}(E)$ from $\rho(E)$, we performed a running average: we choose some odd integer $2r+1$ of the order of 9–25, and then replace each eigenvalue E_i by a local average:

$$E_i' = \frac{1}{2r+1} \sum_{j=i-r}^{i+r} E_j, \tag{3}$$

and $\overline{\rho}(E)$ is approximated by the linear interpolation between the points of coordinates (E_i', i). We compared the results with other methods: one can replace each δ peak in $\rho(E)$ by a Gaussian with a properly chosen mean square deviation. Another method is to discard the low frequency components in a Fourier transform of $\rho(E)$. A detailed explanation and tests of these methods of unfolding are given in Ref. [9]. Note also that for very peculiar spectra it is necessary to break these into parts and to unfold each part separately. Also, the extremal eigenvalues are discarded, since they induce finite size effects. It comes out that of the three methods, the running average unfolding is the best suited in the context of transfer matrices, and it is also the fastest.

B. Symmetries

For quantum Hamiltonians, it is well known that it is necessary to sort the eigenvalues with respect to their quantum numbers, and to compare only eigenvalues of states belonging to the same quantum numbers. This is due to the fact that eigenstates with different symmetries are essentially uncorrelated. The same holds for transfer matrices. In general, a transfer matrix T of a classical statistical mechanics lattice model (vertex model) depends on several parameters (Boltzmann weights w_i). Due to the lattice symmetries, or to other symmetries (permutation of colors and so on), there exist some operators S acting on the same space as the transfer matrix and which are *independent of the parameters*, commuting with T: $[T(\{w_i\}), S] = 0$. It is then possible to find subspaces of T which are also independent of the parameters. Projection on these invariant subspaces amounts to block diagonalizing, T, and to splitting the unique spectrum of T into the many spectra of each block. The construction of the projectors is done with the help of the character table of irreducible representations of the symmetry group. Details can be found in [9,10].

As we will discuss in the next sections, we always restricted ourselves to symmetric transfer matrices. Consequently the blocks are also symmetric, and there are only *real* eigenvalues. The diagonalization is performed using standard methods of linear algebra [contained in the linear algebra package (LAPACK) library]. The construction of the transfer matrix and the determination of its symmetries depend on the model, and are detailed in Sec. III B for the eight-vertex model.

C. Quantities characterizing the spectrum

Once the spectrum has been obtained and unfolded, various statistical properties of the spectrum are investigated. The simplest one is the distribution $P(s)$ of the spacings $s = \epsilon_{i+1} - \epsilon_i$ between two consecutive unfolded eigenvalues. This distribution will be compared to an exponential and to the Wigner law (1). Usually, a simple visual inspection is sufficient to recognize the presence of level repulsion, the main property for nonintegrable models. However, to quantify the ''degree'' of level repulsion, it is convenient to use a parameterized distribution which interpolates between the Poisson law, the Wigner law. From the many possible distributions we have chosen the Brody distribution [2]

$$P_\beta(s) = c_1 s^\beta \exp(-c_2 s^{\beta+1}), \quad (4a)$$

with

$$c_2 = \left[\Gamma\left(\frac{\beta+2}{\beta+1}\right)\right]^{1+\beta} \quad \text{and} \quad c_1 = (1+\beta)c_2. \quad (4b)$$

For $\beta = 0$, this is a simple exponential for the Poisson ensemble, and for $\beta = 1$, one recovers the Wigner surmise for the GOE. This distribution turns out to be convenient, since its indefinite integral can be expressed with elementary functions. It has been widely used in the literature, except when special distributions were expected, as at the metal insulator transition [11]. Minimizing the quantity

$$\phi(\beta) = \int_0^\infty (P_\beta(s) - P(s))^2 ds \quad (5)$$

yields a value of β characterizing the degree of level repulsion of the distribution $P(s)$. We have always found $\phi(\beta)$ to be small. When $-0.1 < \beta < 0.1$, the distribution is close to a Poisson law, while for $0.5 < \beta < 1.2$ the distribution is close to the Wigner surmise.

If a distribution is found to be close to the Wigner surmise (or the Poisson law), this does not mean that the GOE (or the diagonal matrices ensemble) correctly describes the spectrum. Therefore it is of interest to compute functions involving higher order correlations, as, for example, the spectral rigidity [2]

$$\Delta_3(E) = \left\langle \frac{1}{E} \min_{a,b} \int_{\alpha - E/2}^{\alpha + E/2} (N(\epsilon) - a\epsilon - b)^2 d\epsilon \right\rangle_\alpha, \quad (6)$$

where $\langle \rangle_\alpha$ denotes an average over the whole spectrum. This quantity measures the deviation from equal spacing. For a totally rigid spectrum, as that of the harmonic oscillator, one has $\Delta_3^{\text{osc}}(E) = \frac{1}{12}$, for an integrable (Poissonian) system one has $\Delta_3^{\text{Poi}}(E) = E/15$, and for the Gaussian orthogonal ensemble one has $\Delta_3^{\text{GOE}}(E) = (1/\pi^2)[\ln(E) - 0.0687] + \mathcal{O}(E^{-1})$. It has been found that the spectral rigidity of quantum spin systems follows $\Delta_3^{\text{Poi}}(E)$ in the integrable case, and $\Delta_3^{\text{GOE}}(E)$ in the nonintegrable case. However, in both cases, even though $P(s)$ is in good agreement with RMT, deviations from RMT occur for $\Delta_3(E)$ at some system-
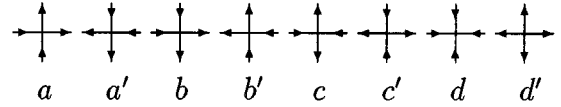

FIG. 2. The Boltzmann weights of the eight vertices.

dependent point E^*. This stems from the fact that the rigidity $\Delta_3(E)$ probes correlations beyond nearest neighbors, in contrast to $P(s)$.

III. ASYMMETRIC EIGHT-VERTEX MODEL ON A SQUARE LATTICE

A. Generalities

We will focus in this section on the asymmetric eight-vertex model on a square lattice. We use the standard notations of Ref. [12]. The eight-vertex condition specifies that only vertices are allowed which have an even number of arrows pointing to the center of the vertex. Figure 2 shows the eight vertices with their corresponding Boltzmann weight. The partition function per site depends on these eight homogeneous variables (or equivalently seven independent values):

$$Z(a, a', b, b', c, c', d, d'). \quad (7)$$

It is customary to arrange the eight (homogeneous) Boltzmann weights in a 4×4 R-matrix:

$$\mathcal{R} = \begin{pmatrix} a & 0 & 0 & d \\ 0 & b & c & 0 \\ 0 & c' & b' & 0 \\ d' & 0 & 0 & a' \end{pmatrix}. \quad (8)$$

The entry $\mathcal{R}_{ij}$ is the Boltzmann weight of the vertex defined by the four digits of the binary representation of the two indices i and j. The row index corresponds to the east and south edges, and the column index corresponds to the west and north edges:

$$\mathcal{R}_{ij} = \mathcal{R}_{\mu\alpha}^{\nu\beta} = w(\mu, \alpha | \beta, \nu),$$

$$\mu \overset{\beta}{\underset{\alpha}{+}} \nu$$

When the Boltzmann weights are unchanged by negating all four edge values, the model is said to be *symmetric*; otherwise it is *asymmetric*. This should not be confused with the symmetry of the transfer matrix. Let us now discuss a general symmetry property of the model. A combinatorial argument [12] shows that for any lattice without dangling ends, the two parameters c and c' can be taken to be equal, and that, for most regular lattices (including the periodic square lattice considered in this work), d and d' can also be taken to be equal (gauge transformation [13]). Specifically, one has

$$Z(a, a', b, b', c, c', d, d')$$

$$= Z(a, a', b, b', \sqrt{cc'}, \sqrt{cc'}, \sqrt{dd'}, \sqrt{dd'}). \quad (9)$$

We will therefore always take $c = c'$ and $d = d'$ in the numerical calculations. In the following, when c' and d' are not mentioned, it is implicitly meant that $c' = c$ and $d' = d$. Let us finally recall that the asymmetric eight-vertex model is equivalent to an Ising spin model on a square lattice, including next nearest neighbor interactions on the diagonals and four-spin interactions around a plaquette (IRF model) [12,14]. However, this equivalence is not exact on a finite lattice, since the $L \times M$ plaquettes do not form a basis (to have a cycle basis, one must take any $L \times M - 1$ plaquettes plus one horizontal and one vertical cycle).

B. Row-to-row transfer matrix

Our aim is to study the full spectrum of the transfer matrix. More specifically, we investigate the properties of the row-to-row transfer matrix which corresponds to building up a periodic $L \times M$ rectangular lattice by adding rows of length L. The transfer matrix T_L is a $2^L \times 2^L$ matrix, and the partition function becomes

$$Z(a,a',b,b',c,d) = \mathrm{Tr}[T_L(a,a',b,b',c,d)]^M. \quad (10)$$

However, there are many other possibilities to build up the lattice, each corresponding to another form of transfer matrix: it just has to lead to the same partition function. Other widely used examples are diagonal (-to-diagonal) and corner transfer matrices [12].

The index of the row-to-row transfer matrix enumerates the 2^L possible configurations of one row of L vertical bonds. We choose a binary coding

$$\alpha = \sum_{i=0}^{L-1} \alpha_i 2^i \equiv |\alpha_0, \ldots, \alpha_{L-1}\rangle, \quad (11)$$

with $\alpha_i \in \{0,1\}$, 0 corresponding to arrows pointing up or to the right and 1 for the other directions. One entry $T_{\alpha,\beta}$ thus describes the contribution to the partition function of two neighboring rows having the configurations α and β:

$$T_{\alpha,\beta} = \sum_{\{\mu\}} \prod_{i=0}^{L-1} w(\mu_i, \alpha_i | \beta_i, \mu_{i+1}). \quad (12)$$

With our binary notation, the eight-vertex condition means that $w(\mu_i, \alpha_i | \beta_i, \mu_{i+1}) = 0$ if the sum $\mu_i + \alpha_i + \beta_i + \mu_{i+1}$ is odd. Therefore, sum (12) reduces to exactly two terms: once μ_0 is chosen (two possibilities), μ_1 is uniquely defined, since α_0 and β_0 are fixed, and so on. For periodic boundary conditions, the entry $T_{\alpha,\beta}$ is zero if the sum of all β_i and α_i is odd. This property naturally splits the transfer matrix into two blocks: entries between row configurations with an even number of up arrows and entries between configurations with an odd number of up arrows.

1. Symmetries of the transfer matrix

Let us now discuss various symmetry properties of the transfer matrix.

(i) When one exchanges the rows α and β, vertices of types a, a', b, and b' will remain unchanged, while vertices of type c and d will exchange into one another. Thus for $c = d$ the transfer matrix $T_L(a,a',b,b',c,d)$ is symmetric. In general the symmetry of the row-to-row transfer matrix is satisfied for $c = d'$ and $d = c'$. In terms of the equivalent IRF Ising model, condition $c = d$ means that the two diagonal interactions J and J' (confer to Ref. [12]) are the same: the Ising model is isotropic, and therefore its row-to-row transfer matrix is symmetric too. This coincidence is remarkable, since the equivalence between the asymmetric eight-vertex model and the Ising model is not exact on a finite lattice, as already mentioned.

(ii) We now consider the effect of permutations of lattice sites preserving the neighboring relations. Denote by S a translation operator defined by

$$S|\alpha_0, \alpha_1, \ldots, \alpha_{L-1}\rangle = |\alpha_1, \ldots, \alpha_{L-1}, \alpha_0\rangle. \quad (13)$$

Then we have

$$\langle \alpha S^{-1} | T_L(a,a',b,b',c,d) | S\beta \rangle$$
$$= \langle \alpha | T_L(a,a',b,b',c,d) | \beta \rangle, \quad (14)$$

and, therefore,

$$[T_L(a,a',b,b',c,d), S] = 0. \quad (15)$$

For the reflection operator R defined by

$$R|\alpha_0, \alpha_1, \ldots, \alpha_{L-1}\rangle = |\alpha_{L-1}, \ldots, \alpha_1, \alpha_0\rangle, \quad (16)$$

we have

$$\langle \alpha R^{-1} | T_L(a,a',b,b',c,d) | R\beta \rangle$$
$$= \langle \alpha | T_L(a,a',b,b',d,c) | \beta \rangle. \quad (17)$$

Thus R commutes with T only for the symmetric case $c = d$:

$$[T_L(a,a',b,b',c,c), R] = 0. \quad (18)$$

Combination of the translations S and the reflection R leads to the dihedral group $\mathcal{D}_L$. These are all the general lattice symmetries in the square lattice case. The one-dimensional nature of the group $\mathcal{D}_L$ reflects the dimensionality of the rows added to the lattice by a multiplication by T. This is general: the symmetries of the transfer matrices of d-dimensional lattice models are the symmetries of $(d-1)$-dimensional space. The translational invariance in the last space direction has already been exploited with the use of the transfer matrix itself, leading to Eq. (10).

(iii) Lastly, we look at symmetries due to operations on the dynamic variables themselves. There is, *a priori*, no continuous symmetry in this model, in contrast with the Heisenberg quantum chain which has a continuous SU(2) spin symmetry. But one can define an operator C returning all arrows:

$$C|\alpha_0, \alpha_1, \ldots, \alpha_{L-1}\rangle = |1-\alpha_0, 1-\alpha_1, \ldots, 1-\alpha_{L-1}\rangle. \quad (19)$$

This leads to an exchange of primed and unprimed Boltzmann weights:

$$\langle \alpha C^{-1} | T_L(a,a',b,b',c,d) | C\beta \rangle$$
$$= \langle \alpha | T_L(a',a,b',b,c,d) | \beta \rangle, \quad (20)$$

TABLE I. The dimensions a_R and degeneracies l_R of the invariant subspaces for $L=14$. R is an arbitrary label of the representations of the dihedral group, and $\exp(ik)$ and λ are the eigenvalues of the corresponding translation and reflection operators (* means that the corresponding representation is not stable under the action of the reflection operator). The two numbers a_R^{even} and a_R^{odd} correspond to the blocks between configurations with an even or odd number of up arrows (see text).

R	k	λ	l_R	a_R^{even}	a_R^{odd}
0	0	1	1	362	325
1	π	-1	1	288	325
2	0	-1	1	234	261
3	π	1	1	288	261
4	$2\pi/7$	*	2	594	585
5	$4\pi/7$	*	2	594	585
6	$6\pi/7$	*	2	594	585
7	$\pi/7$	*	2	576	585
8	$3\pi/7$	*	2	576	585
9	$5\pi/7$	*	2	576	585

Thus for the symmetric eight-vertex model (Baxter model) the symmetry operator C commutes with the transfer matrix:

$$[T_L(a,a,b,b,c,d),C]=0. \tag{21}$$

2. Projectors

Once the symmetries have been identified, it is simple to construct the projectors of one row of each irreducible representation of the group $\mathcal{D}_L$ (details can be found in [9,10]). When L is even, there are four representations of dimension 1 and $L/2-1$ representations of dimension 2 (i.e., in all there are $L/2+3$ projectors). When L is odd, there are two one-dimensional representations and $(L-1)/2$ representations of dimension 2, in all $(L-1)/2+2$ projectors. For the symmetric model with $a=a'$ and $b=b'$, there is an extra $\mathcal{Z}_2$ symmetry which doubles the number of projectors.

Using the projectors block diagonalizes the transfer matrix, leaving a collection of small matrices to diagonalize instead of the large one. For example, for $L=16$, the total row-to-row transfer matrix has the linear size $2^L=65536$, and the projected blocks have linear sizes between 906 and 2065 (see also Tables I and II).

As already mentioned, the block projection not only saves computing time for the diagonalization, but is necessary to sort the eigenvalues with respect to the symmetry of the corresponding eigenstates. In summary, when $c=d$, the row-to-row transfer matrix is symmetric, leading to a real spectrum. Its symmetries have been identified. This is a fortunate situation, since restriction $c=d$ neither prevents nor enforces Yang-Baxter integrability, as will be explained in Sec. III C.

C. Integrability of the eight-vertex model

We now summarize the cases where the partition function of the eight-vertex model can be analyzed and possibly computed. These are the symmetric eight-vertex model, the asymmetric six-vertex model, the free-fermion variety, and some "disorder solutions."

TABLE II. The parameters of the invariant subspaces as in the preceding table for $L=16$.

R	k	λ	l_R	a_R^{even}	a_R^{odd}
0	0	1	1	1162	1088
1	π	-1	1	1033	1088
2	0	-1	1	906	960
3	π	1	1	1033	960
4	$\pi/2$	*	2	2065	2048
5	$\pi/4$	*	2	2062	2048
6	$3\pi/4$	*	2	2062	2048
7	$\pi/8$	*	2	2032	2048
8	$7\pi/8$	*	2	2032	2048
9	$5\pi/8$	*	2	2032	2048
10	$3\pi/8$	*	2	2032	2048

1. Symmetric eight-vertex model

First, in the absence of an "electrical field," i.e., when $a=a',b=b',c=c'$, and $d=d'$, the transfer matrix can be diagonalized using the Bethe ansatz or the Yang-Baxter equations [12]. This case is called the symmetric eight-vertex model, also called the Baxter model [12]. One finds that two row-to-row transfer matrices $T_L(a,b,c,d)$ and $T_L(\bar{a},\bar{b},\bar{c},\bar{d})$ commute if

$$\Delta(a,b,c,d)=\Delta(\bar{a},\bar{b},\bar{c},\bar{d}), \tag{22a}$$

$$\Gamma(a,b,c,d)=\Gamma(\bar{a},\bar{b},\bar{c},\bar{d}), \tag{22b}$$

with

$$\Gamma(a,b,c,d)=\frac{ab-cd}{ab+cd}, \tag{23a}$$

$$\Delta(a,b,c,d)=\frac{a^2+b^2-c^2-d^2}{2(ab+cd)}. \tag{23b}$$

Note that these necessary conditions are valid for *any* lattice size L. One also obtains the *same* conditions for the column-to-column transfer matrices of this model. Thus the commutation relations lead to a foliation of the parameter space in elliptic curves given by the intersection of two quadrics, Eq. (23); that is, to an elliptic parametrization (in the so-called principal regime [12])

$$a=\rho sn(\eta-\nu), \tag{24a}$$

$$b=\rho sn(\eta+\nu), \tag{24b}$$

$$c=\rho sn(2\eta), \tag{24c}$$

$$d=-\rho ksn(2\eta)sn(\eta-\nu)sn(\eta+\nu), \tag{24d}$$

where sn denotes the Jacobian elliptic function, and k their modulus.

It is also well known that the transfer matrix $T(a,b,c,d)$ commutes with the Hamiltonian of the anisotropic Heisenberg chain [15],

$$\mathcal{H} = -\sum_i J_x \sigma_i^x \sigma_{i+1}^x + J_y \sigma_i^y \sigma_{i+1}^y + J_z \sigma_i^z \sigma_{i+1}^z, \quad (25)$$

if

$$1 : \Gamma(a,b,c,d) : \Delta(a,b,c,d) = J_x : J_y : J_z. \quad (26)$$

This means that, given the three coupling constants J_x, J_y, and J_z of a Heisenberg Hamiltonian, there exist infinitely many quadruplets (a,b,c,d) of parameters, such that

$$[T(a,b,c,d), \mathcal{H}(J_x, J_y, J_z)] = 0. \quad (27)$$

Indeed, the three constants J_x, J_y, and J_z uniquely determine η and k in the elliptic parametrization (24), and the spectral parameter ν can take any value, thus defining a continuous one-parameter family. Not only T and $\mathcal{H}$ commute for arbitrary values of the parameter ν, but $\mathcal{H}$ is also related to the logarithmic derivative of T at $\nu = \eta$. In this work, we examine only regions with the extra condition $c = d$ to ensure that T is symmetric, and thus that the spectrum is symmetric. Using the symmetries of the eight-vertex model, one finds that the model (a,b,c,d), with $c = d$ mapped into its principal regime, gives a model $(\bar{a}, \bar{b}, \bar{c}, \bar{d})$ with $\bar{a} = \bar{b}$. In terms of the elliptic parametrization, this means $sn(\eta - \nu) = sn(\eta + \nu)$ or $\nu = 0$.

In summary, in the continuous one-parameter family of commuting transfer matrices $T(\nu)$ corresponding to a given value of Δ and Γ, there are two special values of the spectral parameter ν: $\nu = \eta$ is related to the Heisenberg Hamiltonian $\mathcal{H}(1, \Gamma, \Delta)$, and for $\nu = 0$ the transfer matrix $T(\nu)$ is symmetric (up to a gauge transformation).

2. Six-vertex model

The six-vertex model is a special case of the eight-vertex model: one disallows the last two vertex configurations of Fig. 2, this means $d = d' = 0$. Both the symmetric and asymmetric six-vertex models have been analyzed using the Bethe ansatz or also the Yang-Baxter equations [12,16,17]. We did not examine this situation any further, since condition $c = d$ having a real spectrum [see Sec. III B 1(i)] leads to a trivial case.

3. Free-fermion condition

Another case where the asymmetric eight-vertex model can be solved is the case where the Boltzmann weights verify the so-called *free-fermion* condition

$$aa' + bb' = cc' + dd'. \quad (28)$$

For condition (28), the model reduces to a quantum problem of free fermions, and the partition function can thus be computed [18,19].

The free-fermion asymmetric eight-vertex model is Yang-Baxter integrable; however, the parametrization of the Yang-Baxter equations is more involved compared to the situation described in Sec. III C 1: the row-to-row and column-to-column commutations correspond to two different foliations of the parameter space in algebraic surfaces.

It is also known that the asymmetric eight-vertex free-fermion model can be mapped onto a checkerboard Ising

model. In Appendix A we give the correspondence between the vertex model and the spin model. The partition function per site of the model can be expressed in term of elliptic functions E which are not (due to the complexity of the parametrization of the Yang-Baxter equations) straightforwardly related to the two sets of surfaces parametrizing the Yang-Baxter equations or even to the canonical elliptic parameterization of the generic (non free-fermion) asymmetric eight-vertex model [see Eqs. (35) in the following; see also [25]]. The elliptic modulus of these elliptic functions E is given in Appendix A as a function of the checkerboard Ising variables, as well as in the homogeneous Boltzmann weights $(a, a', b, b', c, c', d,$ and $d')$ for the free-fermion asymmetric eight-vertex model.

Finally, we remark that the restriction $c = d$ is compatible with condition (28) and, in contrast with the asymmetric six-vertex model, the asymmetric free-fermion model provides a case where the row-to-row transfer matrix of the model is symmetric.

4. Disorder solutions

If the parameters $a, a', b, b', c,$ and d are chosen such that the R matrix (8) has an eigenvector which is a pure tensorial product,

$$\mathcal{R} \begin{pmatrix} 1 \\ p \end{pmatrix} \otimes \begin{pmatrix} 1 \\ q \end{pmatrix} = \lambda \begin{pmatrix} 1 \\ p \end{pmatrix} \otimes \begin{pmatrix} 1 \\ q \end{pmatrix}, \quad (29)$$

then the vector

$$\begin{pmatrix} 1 \\ p \end{pmatrix} \otimes \begin{pmatrix} 1 \\ q \end{pmatrix} \otimes \cdots \otimes \begin{pmatrix} 1 \\ p \end{pmatrix} \otimes \begin{pmatrix} 1 \\ q \end{pmatrix} \quad (30)$$

($2L$ factors) is an eigenvector of the diagonal (-to-diagonal) transfer matrix $\widetilde{T}_L$, usually simply called the diagonal transfer matrix. The corresponding eigenvalue is $\Lambda = \lambda^{2L}$, with

$$\lambda = \frac{aa' - bb' + cc' - dd'}{(a+a') - (b+b')}. \quad (31)$$

However, the eigenvalue Λ may, or may not, be the eigenvalue of largest modulus. This corresponds to the existence of so-called disorder solutions [20], for which some dimensional reduction of the model occurs [21]. Condition (29) is simple to express; it reads

$$A^2 + B^2 + C^2 + D^2 + 2AB - 2AD - 2BC - 2CD$$
$$= (A + B - C - D)(a+b)(a'+b') - (A-D)(b^2 + b'^2)$$
$$- (B-C)(a^2 + a'^2), \quad (32)$$

where $A = aa'$, $B = bb'$, $C = cc'$, and $D = dd'$. Note that in the symmetric case $a = a'$, $b = b'$, $c = c'$, and $d = d'$, Eq. (32) factorizes as

$$(a - b + d - c)(a - b + d + c)(a - b - d - c)(a - b - d + c)$$
$$= 0, \quad (33)$$

which is the product of terms giving two disorder varieties and two critical varieties of the Baxter model. It is known that the symmetric model has four disorder varieties (one of

them, $a+b+c+d=0$, is not in the physical domain of the parameter space) and four critical varieties [12]. The missing varieties can be obtained by replacing $\mathcal{R}$ by $\mathcal{R}^2$ in Eq. (29). In our numerical calculations we have always found for the asymmetric eight-vertex model that Λ is either the eigenvalue of largest modulus or the eigenvalue of lowest modulus. Finally, note that condition (32) does *not* correspond to a solution of the Yang-Baxter equations. This can be understood, since disorder conditions like (32) are not invariant under the action of the infinite discrete symmetry group Γ presented in Sec. III D, whereas the solutions of the Yang-Baxter equations are actually invariant under the action of this group [22,23].

On the other hand, similarly to the Yang-Baxter equations, the ''disorder solutions'' can be seen to correspond to families of commuting diagonal transfer matrices $\widetilde{T}_L$ on a subspace V of the 2^{2L}-dimensional space on which $\widetilde{T}_L$ acts,

$$[\widetilde{T}_L(a,a',b,b',c,d),\widetilde{T}_L(\bar{a},\bar{a}',\bar{b},\bar{b}',\bar{c},\bar{d})]|_V=0, \quad (34)$$

where subscript V means that the commutation is only valid on the subspace V. Actually, this subspace is the one-dimensional subspace corresponding to vector (30). The notion of transfer matrices commuting only on a subspace V can clearly have precious consequences on the calculation of the eigenvectors and eigenvalues, and hopefully of the partition function per site. One sees that the Yang-Baxter integrability and the disorder solution ''calculability'' are two limiting cases where V respectively corresponds to the entire space where $\widetilde{T}_L$ acts and to a single vector, namely, Eq. (30).

D. Some exact results on the asymmetric eight-vertex model

When the Boltzmann weights of the model do not verify any of the conditions of Sec. III C, the partition function of the model has not yet been calculated. However, some analytical results can be stated. Algebraic varieties of the parameter space can be presented, which have very special symmetry properties. The intersection of these algebraic varieties with critical manifolds of the model are candidates for multicritical points [24]. We have tested the properties of the spectrum of the transfer matrices on these loci of the phase space.

There actually exists an infinite discrete group of symmetries of the parameter space of the asymmetric eight-vertex model (and, beyond, of the 16-vertex model [25]). The critical manifolds of the model have to be compatible with this group of symmetries, and this is also true for any exact property of the model: for instance, if the model is Yang-Baxter integrable, the Yang-Baxta equations (YBE) are compatible with this infinite symmetry group [22]. However, it is crucial to recall that this symmetry group is not restricted to the Yang-Baxter integrability. It is a symmetry group of the model *beyond* the integrable framework, and provides, for instance, a canonical elliptic foliation of the parameter space of the model (see the concept of quasi-integrability [25]). The group is generated by simple transformations of the homogeneous parameters of the model: the matrix inversion and some representative geometrical symmetries, as, for example, the geometrical symmetry of the square lattice, which amounts to a simple exchange of c and d:

$$t_1 \begin{pmatrix} a & 0 & 0 & d \\ 0 & b & c & 0 \\ 0 & c & b' & 0 \\ d & 0 & 0 & a' \end{pmatrix} = \begin{pmatrix} a & 0 & 0 & c \\ 0 & b & d & 0 \\ 0 & d & b' & 0 \\ c & 0 & 0 & a' \end{pmatrix}.$$

Combining I and t_1 yields an infinite discrete group Γ of symmetries of the parameter space [23]. This group is isomorphic to the infinite dihedral group (up to a semidirect product with $\mathcal{Z}_2$). An infinite-order generator of the nontrivial part of this group is for instance $t_1 I$. In the parameter space of the model this generator yields an infinite set of points located on elliptic curves. The analysis of the orbits of the group Γ for the asymmetric eight-vertex model yields (a finite set of) elliptic curves given by

$$\frac{(aa'+bb'-cc'-dd')^2}{aa'bb'}=\text{const}, \quad \frac{aa'bb'}{cc'dd'}=\text{const} \tag{35}$$

and

$$\frac{a}{a'}=\text{const}, \quad \frac{b}{b'}=\text{const}, \quad \frac{c}{c'}=\text{const}, \quad \frac{d}{d'}=\text{const}.$$

In the limit of the symmetric eight-vertex model one recovers the well-known elliptic curves (23) of the Baxter model given by the intersection of two quadrics. Recalling parametrization (24), one sees that $t_1 I$, the infinite-order generator of Γ, is actually represented as a shift by η of the spectral parameter: $\nu \rightarrow \nu + \eta$.

The group Γ is generically infinite; however, if some conditions on the parameters hold, it degenerates into a finite group. These conditions define algebraic varieties for which the model has a high degree of symmetry. The location of multicritical points seems to correspond to enhanced symmetries, namely, to the algebraic varieties where the symmetry group Γ degenerates into a finite group [24]. Such conditions of commensuration of the shift η with one of the two periods of the elliptic functions occurred many times in the literature of theoretical physics (Tutte-Behara numbers, rational values of the central charge and of critical exponents [26]). Furthermore, from the conformal field theory literature, one can have a prejudice toward free-fermion parastatistics on these algebraic varieties of enhanced symmetry [27]. It is thus natural to concentrate on these. We have therefore determined an *infinite* number of these algebraic varieties, which are remarkably *codimension-1* varieties of the parameter space. Their explicit expressions quickly become very large in terms of the homogeneous parameters of the asymmetric eight-vertex model; however, their expressions are remarkably simple in terms of some algebraic invariants generalizing those of the Baxter model, namely,

$$J_x=\sqrt{aa'bb'}+\sqrt{cc'dd'}, \tag{36a}$$

$$J_y=\sqrt{aa'bb'}-\sqrt{cc'dd'}, \tag{36b}$$

$$J_z=\frac{aa'+bb'-cc'-dd'}{2}. \tag{36c}$$

Note that, in the symmetric subcase, one recovers Eqs. (26). In terms of these well-suited homogeneous variables, it is possible to extend the ''shift doubling'' ($\eta \rightarrow 2\eta$) and ''shift tripling'' ($\eta \rightarrow 3\eta$) transformations of the Baxter model to the asymmetric eight-vertex model. For the shift doubling transformation, one obtains

$$J'_x = J^2_z J^2_y - J^2_x J^2_y - J^2_z J^2_x, \tag{37a}$$

$$J'_y = J^2_z J^2_x - J^2_x J^2_y - J^2_z J^2_y, \tag{37b}$$

$$J'_z = J^2_x J^2_y - J^2_z J^2_x - J^2_z J^2_y, \tag{37c}$$

and for the shift tripling transformation,

$$\begin{aligned} J''_x = (&-2J^2_z J^2_y J^4_x - 3J^4_y J^4_z + 2J^2_y J^4_z J^2_x + J^4_y J^4_x + 2J^4_y J^2_z J^2_x \\ &+ J^4_z J^4_x)J_x, \end{aligned} \tag{38a}$$

$$\begin{aligned} J''_y = (&2J^2_z J^2_y J^4_x - 3J^4_z J^4_x + J^4_y J^4_x - 2J^4_y J^2_z J^2_x + J^4_y J^4_z \\ &+ 2J^2_y J^4_z J^2_x)J_y, \end{aligned} \tag{38b}$$

$$\begin{aligned} J''_z = (&J^4_y J^4_z + 2J^4_y J^2_z J^2_x - 3J^4_y J^4_x - 2J^2_y J^4_z J^2_x + 2J^2_z J^2_y J^4_x \\ &+ J^4_z J^4_x)J_z. \end{aligned} \tag{38c}$$

The simplest codimension-1 finite order varieties are $J_x=0$, $J_y=0$, or $J_z=0$. One remarks that $J_z=0$ is nothing but the free-fermion condition (28), which is thus a condition for Γ to be finite. Another simple example is

$$J_y J_z - J_x J_y - J_x J_z = 0, \tag{39}$$

and the relations obtained by all permutations of x, y, and z. Using the two polynomial transformations (37) and (38), one can easily obtain an *infinite number* of codimension-1 algebraic varieties of finite order. The demonstration that the codimension-1 algebraic varieties built in such a way are actually finite-order conditions of Γ will be given elsewhere. Some low-order varieties are given in Appendix B. In Sec. IV, the lower-order varieties are tested from the view point of statistical properties of the transfer matrix spectrum.

IV. RESULTS OF THE RMT ANALYSIS

A. General remarks

The phase space of the asymmetric eight-vertex model with the constraint $c=d$ (ensuring symmetric transfer matrices and thus real spectra) is a four-dimensional space (five homogeneous parameters a, a', b, b', and c). Many particular algebraic varieties of this four-dimensional space have been presented in Sec. III, and will now be analyzed from the random matrix theory point of view. We will present the full distribution of eigenvalue spacings and the spectral rigidity at some representative points. Then we will analyze the behavior of the eigenvalue spacing distribution along different paths in the four-dimensional parameter space. These paths will be defined, keeping some Boltzmann weights constant and parameterizing the others by a single parameter t.

We have generated transfer matrices for various linear sizes, up to $L=16$ vertices, leading to transfer matrices of size up to 65536×65536. Tables I and II give the dimensions of the different invariant subspaces for $L=14$ and 16. Note that the size of the blocks to diagonalize increases exponentially with the linear size L. The behavior in the various subspaces is not significantly different. Nevertheless the statistics is better for larger blocks, since the influence of the boundary of the spectrum and finite size effects are smaller. To obtain better statistics, we also averaged the results of several blocks for the same linear size L.

B. Near the symmetric eight-vertex model

Figure 3 presents the probability distribution of the eigenvalue spacings for three different sets of Boltzmann weights which are listed in Table III. Figure 3(a) corresponds to a point of a symmetric eight-vertex model, while Figs. 3(b) and 3(c) are results for the asymmetric eight-vertex model. The data points result from about 4400 eigenvalue spacings coming from the ten even subspaces for $L=14$ which are listed in Table I. For the symmetric model (a), using the symmetry under reversal of all arrows, these blocks can once more be split into two sub-blocks of equal size. The broken lines show the exponential and the Wigner distribution as the exact results for the diagonal random matrix ensemble (i.e., independent eigenvalues) and the 2×2 GOE matrices. In Fig. 3(a) the data points fit very well an exponential, whereas in Figs. 3(b) and 3(c) they are close to the Wigner surmise. In the latter cases we have also added the best fitting Brody distribution with the parameter β listed in Table III. The agreement with the Wigner distribution is better for case (c), where the asymmetry expressed by the ratio a/a' is larger.

We also have calculated the spectral rigidity to test how accurate is the description of spectra of transfer matrices in terms of spectra of mathematical random matrix ensembles. In Fig. 4 we present the spectral rigidity $\Delta_3(E)$ for the same points in parameter space corresponding to integrability and to nonintegrability as in Fig. 3. The two limiting cases corresponding to the Poissonian distributed eigenvalues (solid line) and to GOE distributed eigenvalues (dashed line) are also shown. For the integrable point the agreement between the numerical data and the expected rigidity is very good. For the nonintegrable case the departure of the rigidity from the expected behavior appears at $E \approx 2$ in case (b) and at $E \approx 6$ in case (c) (in units of eigenvalue spacings), indicating that the RMT analysis is only valid on short scales. Such behavior has already been seen in quantum spin systems [5,7]. We stress that the numerical results concerning the rigidity depend much more on the unfolding than the results concerning the spacing distribution.

Summarizing the results for the eigenvalue spacing distribution and the rigidity, we found very good agreement with the Poissonian ensemble for the symmetric eight-vertex model (a), good agreement with the GOE for the asymmetric model (c), and some intermediate behavior for the asymmetric eight-vertex model (b). The difference between the behavior for cases (b) and (c) can be explained by the larger asymmetry in case (c): case (b) is closer to the integrable symmetric eight-vertex model.

To study the proximity to the integrable model, we determined the ''degree'' of level repulsion β by fitting the Brody distribution to the statistics along a path
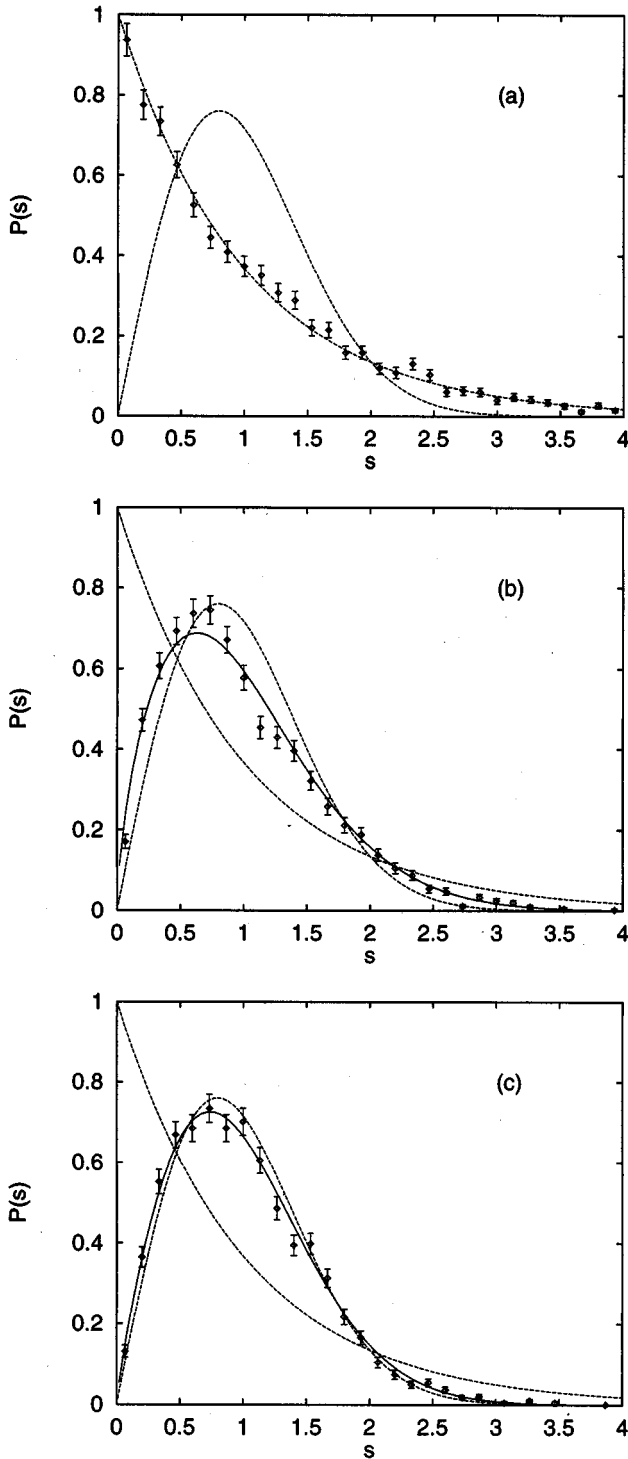
FIG. 3. The distribution $P(s)$ of eigenvalue spacings for the three sets of Boltzmann weights enumerated in Table III. The continuous lines give the exponential for a Poissonian spectrum and the Wigner distribution (1) for the GOE, the broken lines in figures (b) and (c) are the fitted Brody distribution with the β given in Table III.

$(a=t, \ a'=4/t, \ b=b'=4/5,$ and $c=\sqrt{5/8})$ joining cases (a) and (c) for different lattice sizes. The result is shown in Fig. 5; the details about the number of blocks and eigenvalue spacings used in the distributions are listed in Table IV. A finite size effect is seen: we always find $\beta \approx 0$ for the sym-

TABLE III. The Boltzmann weights for the three cases of Figs. 3 and 4. The last column indicates the parameter β of the Brody distribution shown in Fig. 3.

Case	a	a'	$b=b'$	$c=d$	β
(a)	2	2	0.8	$\sqrt{5/8} \approx 0.790569$	0.02
(b)	1.8	2.2222	0.8	$\sqrt{5/8} \approx 0.790569$	0.64
(c)	1.6	2.5	0.8	$\sqrt{5/8} \approx 0.790569$	0.85

metric model at $a/a'=1$, and increasing the system size leads to a better coincidence with the Wigner distribution ($\beta=1$) for the nonintegrable asymmetric model $a \neq a'$. So in the limit $L \to \infty$ we claim to find a δ peak at the symmetric point $a=a'=2$. We also found that the size effects are really controlled by the length L and not by the size of the block. However, our finite size analysis is only qualitative. There is an uncertainty on β of about ± 0.1. There are two possible sources for this uncertainty. The first one is a simple statistical effect, and could be reduced by increasing the number of spacings. The second one is a more inherent problem due to the empirical parameters in the unfolding procedure. This source of errors cannot be suppressed increasing the size L. For a quantitative analysis of the finite size effects it would be necessary to have a high accuracy of β and to vary L over a large scale, which is not possible because of the exponential growth of the block sizes with L.

To test a possible extension of the critical variety $a=b+c+d$ outside the symmetric region $a=a'$, $b=b'$, we performed similar calculations along the path ($a=t$, $a'=4/t$, $b=b'=\frac{4}{5}$, and $c=\frac{3}{5}$) crossing the symmetric integrable variety at a critical point $t=2$. The results are the same: we did not find any kind of Poissonian behavior when $t \neq 2$. We tested one single path and not the whole neighborhood around the Baxter critical variety. This would be necessary if one really wanted to test a possible relation between Poissonian behavior and criticality instead of integrability (both properties often being related). The possible relation between Poissonian behavior and criticality will be discussed for spin models in the second paper. We conclude, from all these calculations, that the analysis of the properties of the unfolded spectrum of transfer matrices provides an efficient way to detect integrable models, as already known for the energy spectrum of quantum systems [3–6].

C. Case of Poissonian behavior for the asymmetric eight-vertex model

We now investigate the phase space far from the Baxter model. We define paths in the asymmetric region which cross the varieties introduced above but which do not cross the Baxter model. These paths and their intersection with the different varieties are summarized in Table V. Figure 6 corresponds to path (a) ($a=\frac{4}{5}$, $a'=\frac{5}{4}$, $b=b'=t$, and $c=1.3$). This defines a path which crosses the free-fermion variety at the solution of Eq. (28): $t=t_{ff}=\sqrt{2.38}$; and the disorder variety at the two solutions of Eq. (29): $t=t_{di}^{max} \approx 1.044$ and at $t=t_{di}^{min} \approx 1.0056$ (the subscript ''di'' stands for disorder). See Table V for the intersections with the other varieties. We have numerically found that, at the point $t=t_{di}^{max}$, eigenvalue (31) is the one of largest modulus, whereas at $t=t_{di}^{min}$ it is the
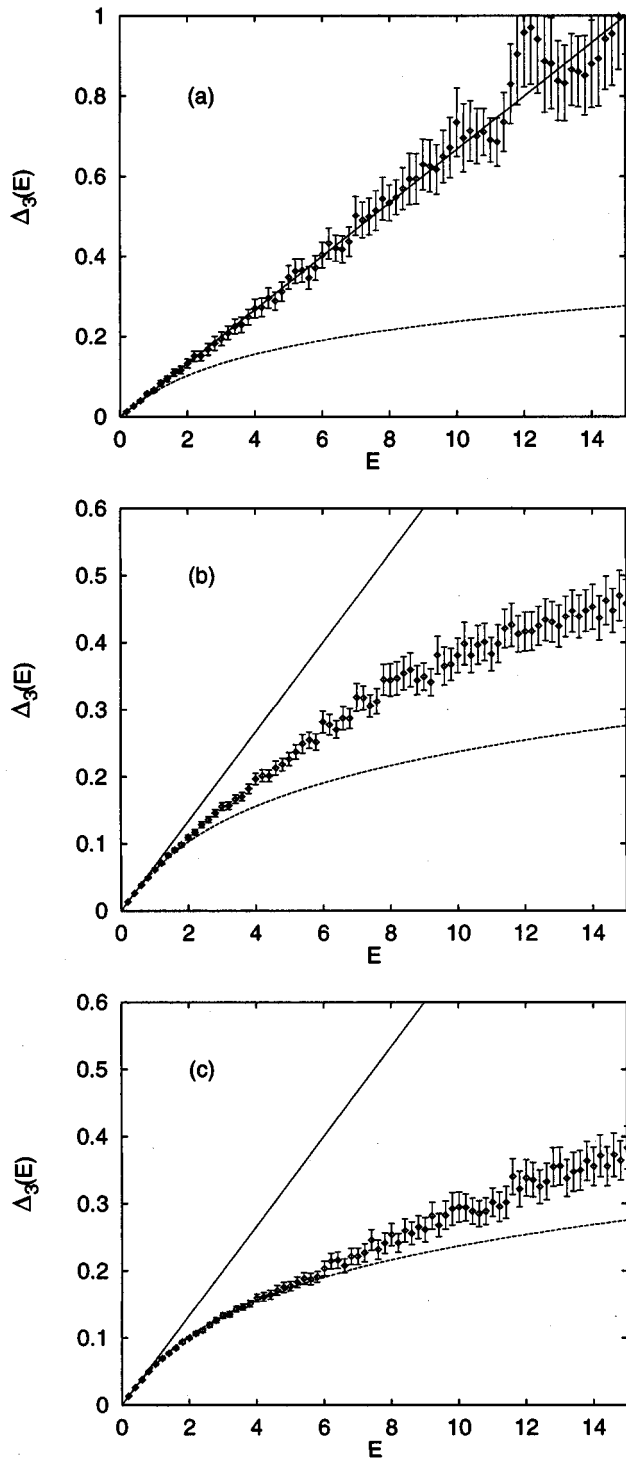
FIG. 4. The spectral rigidity $\Delta_3(E)$ for the three sets of Boltz-mann weights enumerated in Table III. The lines give the limiting case for a Poissonian spectrum and for the GOE.
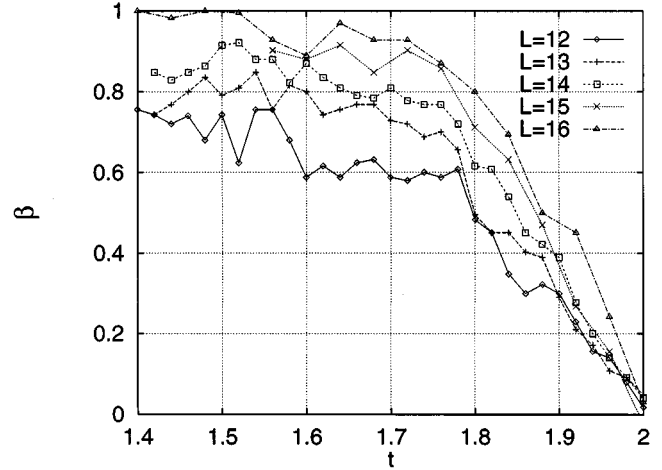

FIG. 5. The degree of level repulsion β obtained by a fit of the eigenvalue spacing distribution $P(s)$ to the Brody distribution for lattice sizes $L=12,\ldots,16$. The Boltzmann weights vary along the path ($a=t$, $a'=4/t$, $b=b'=4/5$, $c=d=\sqrt{5/8}$) which gives a symmetric model for $t=2$. The number of spacings used for each size is given in Table IV.

β is close to zero. This is not surprising for $t=t_{\mathrm{ff}}$ since the model is Yang-Baxter integrable at this point. The value $\beta(t_{\mathrm{ff}})$ is slightly negative: this is related to a ''level attrac-tion'' already noted in [8]. The downward peak is very sharp and a good approximation of a δ peak that we expect for an infinite size. At $t=t_{\mathrm{di}}^{\min}$ and $t=t_{\mathrm{di}}^{\max}$ the model is *not* Yang-Baxter integrable. We cannot numerically resolve between these two points. Therefore, we now study paths where these two disorder solutions are clearly distinct. For Fig. 8 they are both below the free-fermion point, while for Fig. 7 the free-fermion point is between the two disorder solution points.

In both Figs. 7 and 8, we show the results for two paths which differ only by an exchange of the two weights $a \leftrightarrow a'$. In Fig. 7 one clearly sees a peak to β slightly nega-tive at the free-fermion point at $t=0.8$, and another one at one disorder solution point $t=t_{\mathrm{di}}^{\max}\approx 1.46$ for both curves but no peak at the second disorder solution point $t=t_{\mathrm{di}}^{\min}\approx 0.55$. It is remarkable that only point $t=t_{\mathrm{di}}^{\max}$ yields the eigenvalue of largest modulus for the diagonal (-to-diagonal) transfer matrix. Consequently, one has the partition function per site of the model at this point. At point $t=t_{\mathrm{di}}^{\min}$, where the parti-tion function is not known, we find level repulsion. How-ever, only for path (c) is the degree of level repulsion β close to unity, while for path (b) it saturates at a much smaller value. Another difference between cases (b) and (c) is a minimum in the curve of $\beta(t)$ for path (c) at $t\approx 1.8$ which is

eigenvalue of smallest modulus (this is the superscript min or max). The results shown are obtained using the representa-tion $R=0$ for $L=16$ (see Table II). After unfolding and dis-carding boundary states we are left with a distribution of about 1100 eigenvalue spacings. One clearly sees that, most of the time, β is of order 1, signaling that the spacing distri-bution is very close to the Wigner distribution, except for $t=t_{\mathrm{ff}}\approx 1.54$ and for t close to the disorder solutions, where

TABLE IV. Numbers of representations and their dimensions used for the distributions leading to Fig. 5.

L	Dimension a_j of the blocks	No. (spacings)
12	122, 176, 174, 166, 165,165	870
13	190, 315, 315, 315	1000
14	362, 596, 596, 576	2000
15	612, 1092, 1094	2600
16	1162, 1088, 2065	4000

TABLE V. The parametrization of the paths (a)–(e) and their intersection points with the different algebraic varieties (see text).

	(a)	(b)	(c)	(d)	(e)
a	0.8	0.4	2	1.2	0.8
a'	1.25	2	0.4	0.8	1.2
b	t	t	t	t	t
b'	t	1.5	1.5	1.5	1.5
$c=d$	1.3	1	1	1.3	1.3
t_{ff}	1.5427	0.8	0.8	1.6133	1.6133
$t_{\text{di}}^{\min}$	1.0057	0.5520	0.5520	0.6156	0.6156
$t_{\text{di}}^{\max}$	1.0443	1.4608	1.4608	0.2424	0.2424
t_{fo}^{6}	1.3	0.6667	0.6667	1.1267	1.1267
t_{fo}^{6}	1.5991	0.8141	0.8141	1.7474	1.7474
t_{fo}^{8}	1.6000	0.8141	0.8141	1.7001	1.7001
t_{fo}^{16}		0.5237	0.5237	0.6337	0.6337

FIG. 7. The degree of level repulsion β for paths (b) and (c) (see Table V) [$L=16$ and 1000 spacings for (b) and 3000 for (c)].

not seen for path (b). We do not yet have a theoretical explanation for these phenomena: these points are not located on any of the varieties presented in this paper. We stress that an explanation cannot be found straightforwardly in the framework of the symmetry group Γ presented here, since a and a' appear only with the product aa'. It also cannot be found in the Yang-Baxter framework, since a and a' are on the same footing in the Yang-Baxter equations.

In Fig. 8 the curves of β for the two paths (d) and (e) again coincide very well at the free-fermion point at $t=t_{\text{ff}}\approx1.61$. But the behavior is very different for $t<1$, where the solutions of the disorder variety are located. For path (d) neither of the two disorder points is seen on the curve $\beta(t)$, which is almost stationary near a value around 0.6. This means that some eigenvalue repulsion occurs, but the entire distribution is not very close to the Wigner surmise. Conversely, for path (e) the spacing distribution is very close to a Poissonian distribution [$\beta(t)\approx0$] when t is between the two disorder points. This suggests that the status of eigenvalue spectrum on the disorder variety of the asymmetric eight-vertex model is not simple: a more systematic study would help to clarify the situation.
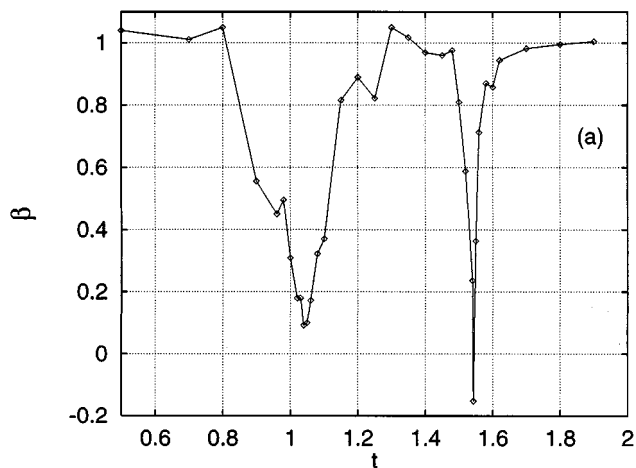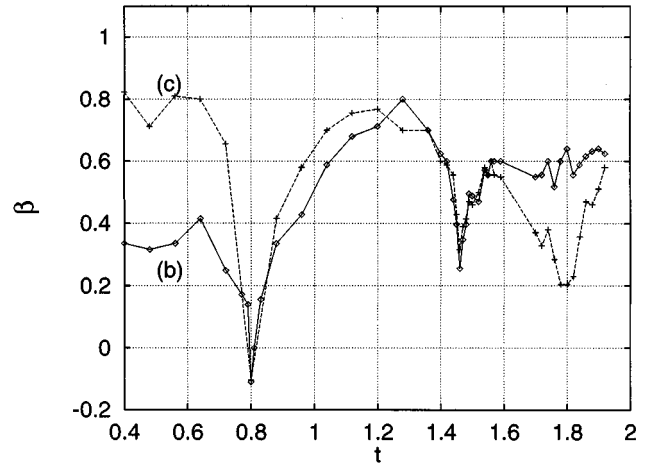
We now summarize the results from Figs. 6–8: generally, the statistical properties of the transfer matrix spectra of the asymmetric eight-vertex model are close to those of the GOE except for some algebraic varieties. We always have a very sharp peak with $\beta\to0$ at the free-fermion point, often $\beta\approx-0.2$. All other points with $\beta\to0$ are found to be a solution of the disorder variety (32) of the asymmetric eight-vertex model.

D. Special algebraic varieties

To conclude this section, we discuss the special algebraic varieties of the symmetry group Γ. As explained in Sec. III D, it is possible to construct an infinite number of algebraic varieties where the generator is of finite order n: $(t_1 I)^n=Id$, and thus Γ is finite order. As an example, the solutions for $n=6$ and 16 are given in Appendix B. We have actually calculated a third variety, the expression of which is too long to be given ($n=8$). In Table V we give the values of the parameter t for which each path crosses each variety t_{fo}^6, t_{fo}^8, and t_{fo}^{16} (the subscript "fo" stands for finite order, and the superscript is the order f). It is easy to verify on the different curves that no tendency to Poissonian behavior oc-
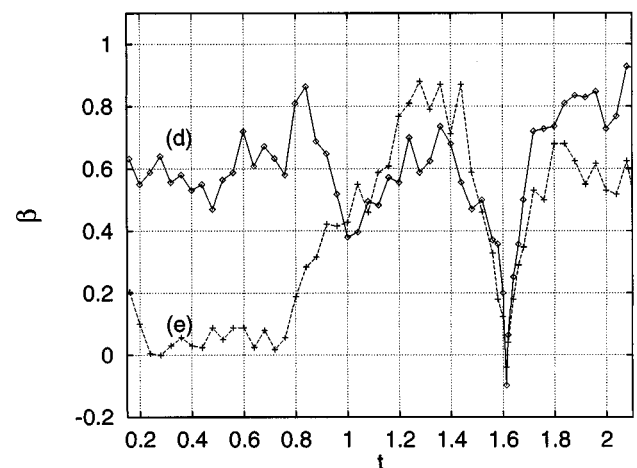

FIG. 6. The degree of level repulsion β for path (a) (see Table V) ($L=16$ and 1000 spacings).

FIG. 8. The degree of level repulsion β for paths (d) and (e) (see Table V) ($L=14$ and about 2000 spacings).

curs at these points. We therefore give a negative answer to the question of a special status of *generic* points of the algebraic finite-order varieties with respect to the statistical properties of the transfer matrix spectra. However, one can still imagine that subvarieties of these finite-order varieties could have Poissonian behavior and be candidates for free parafermions or multicritical points.

V. CONCLUSION AND DISCUSSION

We have found that the entire spectrum of the symmetric row-to-row transfer matrices of the eight-vertex model of lattice statistical mechanics is sensitive to the Yang-Baxter integrability of the model. The GOE provides a satisfactory description of the spectrum of non-Yang-Baxter integrable models: the eigenvalue spacing distribution and the spectral rigidity up to an energy scale of several spacings are in agreement with the Wigner surmise and the rigidity of the GOE matrix spectra. This accounts for ''eigenvalue repulsion.'' In contrast, for Yang-Baxter integrable models, the unfolded spectrum has many features of a set of independent numbers: the spacing distribution is Poissonian and the rigidity is linear over a large energy scale. This accounts for ''eigenvalue independence.'' However, we have also given a non-Yang-Baxter integrable disorder solution of the asymmetric eight-vertex model. For some parts of it the spectrum is clearly Poissonian, too. This suggests that the Wignerian nature of the spectrum is not completely controlled by the Yang-Baxter integrability alone, but possibly by a more general notion of ''calculability,'' possibly based on the existence of a family of transfer matrices commuting on the same subspace. We have also found some ''eigenvalue attraction'' for some Yang-Baxter integrable models, namely, for most points of the free-fermion variety. These results could be a surprise, since we do not *a priori* expect properties involving all the 2^L eigenvalues when only the few eigenvalues of larger modulus have a physical significance. However, the eigenvalues of small modulus control the finite size effects, and it is well known that, for example, the critical behavior (critical exponents) can be deduced from the finite size effects. The nature of the eigenvalue spacing distribution being an effective criterion, we have also used it to test unsuccessfully various special manifolds including the vicinity of the critical variety of the Baxter model. In a forthcoming publication we will present a similar study of a spin model (rather than vertex models). In particular, it is interesting to analyze the spectrum on a critical, but not Yang-Baxter integrable, algebraic variety of codimension 1, as it can be found in the $q = 3$ Potts model on a triangular lattice with three-spin interactions [28]. However, this leads to models, the transfer matrix of which cannot be made symmetric. This will require

a particular study of complex spectra which is much more complicated. In particular the eigenvalue repulsion becomes two dimensional, and to investigate the eigenvalue spacing distribution one has to analyze the distances between eigenvalues in two dimensions.

APPENDIX A

Hereafter we give the correspondence between the asymmetric eight-vertex model on the free-fermion variety and the checkerboard Ising model. The vertex model is specified by eight homogeneous parameters. The gauge invariance (9), together with the free-fermion condition (28), leads to only four independent parameters. The checkerboard model is specified by the four independent usual low-temperature variables $x_i = e^{-K_i}$:

$$a = \frac{1}{2}\left(x_1 x_2 x_3 x_4 + \frac{1}{x_1 x_2 x_3 x_4}\right), \quad a' = \frac{1}{2}\left(\frac{x_1 x_3}{x_2 x_4} + \frac{x_2 x_4}{x_1 x_3}\right),$$
$$(A1)$$

$$b = \frac{1}{2}\left(\frac{x_1 x_4}{x_2 x_3} + \frac{x_2 x_3}{x_1 x_4}\right), \quad b' = \frac{1}{2}\left(\frac{x_1 x_2}{x_4 x_3} + \frac{x_4 x_3}{x_1 x_2}\right), \quad (A2)$$

$$c = \frac{1}{2}\left(\frac{x_1 x_2 x_3}{x_4} + \frac{x_4}{x_1 x_2 x_3}\right), \quad c' = \frac{1}{2}\left(\frac{x_1 x_4 x_3}{x_2} + \frac{x_2}{x_1 x_4 x_3}\right),$$
$$(A3)$$

$$d = \frac{1}{2}\left(\frac{x_4 x_3 x_2}{x_1} + \frac{x_1}{x_4 x_3 x_2}\right), \quad d' = \frac{1}{2}\left(\frac{x_1 x_4 x_2}{x_3} + \frac{x_3}{x_1 x_4 x_2}\right).$$
$$(A4)$$

The modulus k_{check} of the checkerboard Ising model, or, equivalently, of the asymmetric eight-vertex model, reads

$$k_{\text{check}}^2 = \frac{k_N}{k_D}, \qquad (A5)$$

with

$$k_N = 16(x_3^2 x_2^2 x_1^2 + x_4^2) \times \text{ circular permutations,}$$

$$k_D = (x_1^2 x_2^2 x_3^2 x_4^2 - x_1^2 x_2^2 - x_1^2 x_3^2 + x_1^2 x_4^2 + x_3^2 x_4^2 + x_4^2 x_2^2 - x_3^2 x_2^2$$
$$-1) \times \text{ (circular permutations),}$$

or, equivalently,

$$k_{\text{free}}^2 = \frac{16 c' d' c d}{16 c' d' c d - 8a' b a b' - 2a'^2 b^2 - 2a^2 b'^2 - 2a^2 b^2 - 2b'^2 a'^2 + (a^2 - a'^2)^2 + (b^2 - b'^2)^2}. \qquad (A6)$$

APPENDIX B

In this appendix we give some algebraic varieties where the group Γ becomes *finite*. Two varieties of order 6 $[(t_1 I)^6 = Id]$,

$$a_{\pm} = \frac{cd^3 \pm c^2 d^2 + dc^3 - cdbb'}{a'dc \pm a'bb'} \tag{B1}$$

and a variety of order 16 $[(t_1 I)^{16} = Id]$,

$$(u^2 - v^2)(u - v) + uv(u^2 + v^2) = 0, \tag{B2}$$

with

$$u = \frac{cc'dd'(aa' + bb' - c^2 - d^2)^2}{(aa'bb - cc'dd')^2} - 1 = \left(\frac{J_x J_z - J_y J_z}{J_x J_y} \right)^2 - 1, \tag{B3}$$

$$v = \frac{aa'bb'(aa' + bb' - c^2 - d^2)^2}{(aa'bb - cc'dd')^2} - 1 = \left(\frac{J_x J_z + J_y J_z}{J_x J_y} \right)^2 - 1. \tag{B4}$$

[1] E. P. Wigner, Ann. Math. **62**, 548 (1955); **65**, 203 (1957); **67**, 325 (1958).

[2] M. L. Mehta, *Random Matrices*, 2nd ed. (Academic, San Diego, 1991).

[3] D. Poilblanc, T. Ziman, J. Bellisard, F. Mila, and G. Montambaux, Europhys. Lett. **22**, 537 (1993).

[4] T. C. Hsu and J.-C. Anglès d'Auriac, Phys. Rev. B **47**, 14 291 (1993).

[5] G. Montambaux, D. Poilblanc, J. Bellisard, and C. Sire, Phys. Rev. Lett. **70**, 497 (1993).

[6] P. van Ede van der Pals and P. Gaspard, Phys. Rev. E **49**, 79 (1994).

[7] H. Bruus and J.-C. Anglès d'Auriac, Europhys. Lett. **35**, 321 (1996).

[8] H. Meyer, J.-C. Anglès d'Auriac, and H. Bruus, J. Phys. A: Math. Gen. L (1996).

[9] H. Bruus and J.-C. Anglès d'Auriac, Phys. Rev. B **55**, 9142 (1997).

[10] H. Meyer, Ph.D. thesis, Univ. J. Fourier, Grenoble, France, 1996.

[11] I. Varga, E. Hofstetter, M. Schreiber, and J. Pipek, Phys. Rev. B **52**, 7783 (1995).

[12] R. Baxter, *Exactly Solved Models in Statistical Mechanics* (Academic, New York, 1982).

[13] A. Gaaf and J. Hijmans, Physica A **80**, 149 (1975).

[14] P. W. Kasteleyn, in *Fundamental Problems in Statistical Mechanics III, Proceedings of the 1994 Wageningen Summer School*, edited by E. Cohen (North-Holland, Amsterdam, 1975), pp. 103–155.

[15] B. Sutherland, J. Math. Phys. **11**, 3183 (1970).

[16] E. H. Lieb and F. Y. Wu, in *Phase Transitions and Critical Phenomena*, edited by C. Domb and M. Green (Academic, New York, 1972), Vol. 1, pp. 331–490.

[17] I. M. Nolden, J. Stat. Phys. **67**, 155 (1992).

[18] C. Fan and F. Y. Wu, Phys. Rev. B **2**, 723 (1970).

[19] B. U. Felderhof, Physica **66**, 509 (1973).

[20] M. T. Jaekel and J.-M. Maillard, J. Phys. A **18**, 1229 (1985).

[21] A. Georges, D. Hansel, P. Le Doussal, and J.-M. Maillard, J. Phys. **A20**, 5299 (1987).

[22] M. P. Bellon, J.-M. Maillard, and C.-M. Viallet, Phys. Lett. B **260**, 87 (1991).

[23] J.-M. Maillard, J. Math. Phys. **27**, 2776 (1986).

[24] H. Meyer, J.-C. Anglès d'Auriac, J.-M. Maillard, and G. Rollet, Physica A **209**, 223 (1994).

[25] M. Bellon, J.-M. Maillard, and C.-M. Viallet, Phys. Lett. B **281**, 315 (1992).

[26] J.-M. Maillard and R. Rammal, J. Phys. **A16**, 353 (1983).

[27] See, for example, S. Dasmahapatra, R. Dedem, T. R. Klassen, B. M. McCoy, and E. Melzer, in *Proceedings of the Conference on Yang-Baxter Equations in Paris*, edited by J.-M. Maillard (World Scientific, Singapore, 1993).

[28] F. Y. Wu and R. K. P. Zia, J. Phys. A **14**, 721 (1981).